International Journal of Agriculture Innovations and Research
Volume 6, Issue 2, ISSN (Online) 2319-1473
Manuscript Processing Details (dd/mm/yyyy) :
Received: 21/08/2017 | Accepted on: 28/08/2017 | Published: 07/09/2017

Green Synthesis, Characterization of Iron Oxide Nanoparticles using Leucas Aspera Leaf Extract and Evaluation of Antibacterial and Antioxidant Studies

Veeramanikandan V[1*], Madhu G. C.[1], Pavithra V[1], Jaianand K[2] and Balaji P[2]
[1]PG & Research centre in Microbiology, MGR College, Dr. MGR Nagar, Hosur, Tamil Nadu, India - 635109.
[2]PG & Research centre in Biotechnology, MGR College, Dr. MGR Nagar, Hosur, Tamil Nadu, India - 635109.
*Corresponding author email id: vra.manikandan@gmail.com

Abstract **– An eco-friendly green synthesis of iron oxide nanoparticles using leaf extract of *Leucas aspera* was investigated. The characteristics of the obtained Fe3O4 nanoparticles were studied using UV-Visible spectrophotometer, FTIR, SEM with EDX, XRD and HPLC. The synthesized Iron oxide nanoparticles were effectively utilized for the antibacterial activity and antioxidant studies. The maximum zone of inhibition was found to be high in Gram negative bacteria when compared to Gram positive bacteria. This green method of synthesizing Fe3O4 nanoparticles could also be extended to fabricate other industrially important metal oxides. This simple, low cost and greener method for development of nanoparticles may be valuable in environmental, biotechnological and biomedical applications. Thus the present study proven the biological approach of synthesis of Iron oxide nanoparticles using *Leucas aspera* leaf extract appears to be ecofriendly and cost effective alternative to conventional chemical and physical methods and would be suitable for developing large scale production. As a result, the green synthesis using *Leucas aspera* leaf extracts can be economic and effective method for the synthesis of iron oxide nanoparticles.**

Keywords **– Antibacterial, Antioxidant, Green Synthesis, Iron Oxide Nanoparticles, Leucas Aspera.**

I. INTRODUCTION

Nanotechnology can be defined as the manipulation of matter through certain chemical and physical processes to create materials with specific properties, which can be used in particular applications. A nanoparticle can be defined as a microscopic particle that has at least one dimension less than 100 nanometers in size [1]. Unlike bulk materials, they have unique optical, thermal, electrical, chemical and physical properties [2] and hence, they find a variety of applications in the areas of medicine, chemistry, environment, energy, agriculture, information, and communication, heavy industry, and consumer goods. Nanoparticles, because of their small size, have distinct properties compared to the bulk form of the same material, thus offering many new developments in the fields of biosensors, biomedicine and bio nanotechnology.

Nanotechnology is also being utilized in medicine for diagnosis, therapeutic drug delivery and for the development of treatment for many diseases and disorders specifically in the areas of drug delivery, as medical diagnostic tools, as cancer treatment agents (Gold, Cu, Fe nanoparticles) etc. During the last two decades, the biosynthesis of metal nanoparticles (silver, copper, iron, gold, platinum and palladium) has received considerable attention due to the growing need to develop environmentally sociable technologies in material synthesis.

The biological synthesis of nanoparticle is a challenging concept which is very well known as green synthesis. Biosynthesis of nanoparticles could be an alternative to traditional chemical methods for the production of metallic nanomaterials in a clean, nontoxic and ecologically sound manner. Green synthesis of nanoparticle is cost effective, easily available, eco friendly, non toxic, large scale production can be done easily and act as reducing and capping agent when compared to the chemical method which is a very costly as well as emits hazardous by products which can have some deleterious effects on the environment. Synthesis of nanoparticles using plants provides more biocompatible nanoparticles than chemical synthesis, whereas chemical synthesis may lead to the presence of some toxic chemical species on the surface of nanoparticles that may have undesirable effects in biomedical applications [3].

Plant-mediated biological synthesis of nanoparticles has gained importance only in the recent years [4]. Plant extracts reduce the metal ions in a shorter time as compared to microbes. Depending upon plant type and concentration of phytochemicals, nanoparticles are synthesized within a few minutes or hours [5].

Iron oxide nanoparticles have attracted intensive research interest because of their important applications in cancer therapy, drug delivery, magnetic resonance imaging (MRI) and wastewater treatment [6]. Iron based nanoparticles are of great interest because of low cost, availability and properties possessed are similar to that of other metallic nanoparticles and find applications in heat transfer systems as super strong materials, sensors, antimicrobial, bactericidal agents used to coat hospital equipment and also as catalysts. The biosynthesis of iron oxide nanoparticles of different sizes and shapes has been reported using bacteria [7], fungi [8] and plant extract [9].

II. MATERIALS AND METHODS

A. Material

Leucas aspera (Willd.) Linn. (Family: Lamiaceae) commonly known as 'Thumbai' [10] is distributed throughout India from the Himalayas down to Ceylon. The plant is used traditionally as an antipyretic and insecticide. Flowers are valued as stimulant, expectorant, aperient, diaphoretic, insecticide and emmenagogue. Leaves are

considered useful in chronic rheumatism, psoriasis and other chronic skin eruptions. Bruised leaves are applied locally in snake bites.

Collection of Plant Material

The whole plants of *Leucas aspera* were collected from MGR College, Hosur Tamil Nadu state, India during the month of December 2016. The collected plants were identified [11] and authenticated. The collected leaf material was tightly packed with polyethene bag and then transferred to the laboratory. Then the leaves were washed with distilled water twice and kept under room temperature.

Pure Culture

The bacterial strains *Escherichia coli* (NCIM 2065), *Pseudomonas aeruginosa* (NCIM 2036), *Salmonella enterica* (NCIM 5256), *Shigella flexneri* (NCIM 5265), *Staphlococcus aureus* (NCIM 2901), *Vibrio cholera* (NCIM 5316), *Bacillus cereus* (NCIM 2217), *Listeria monocytogenes* (NCIM 5277), *Proteus mirabilis* (NCIM232), *Klebsiella sp* (NCIM 2690) used in this study were obtained from the National Collection of Industrial Microorganisms (NCIM), CSIR – National Chemical Laboratory, Pune, India. They were maintained on nutrient agar slants at 4 °C and were sub cultured every 15 days to maintain its viability.

B. Methods

Preparation of Plant Leaf Extract

Twenty five grams of *Leucas aspera* leaves were accurately weighed and thoroughly washed under running tap water and followed by washing it with double distilled water to remove surface impurities. They were crushed using a mortar and pestle and finely macerated. After homogenization, 100 ml of deionised water was added and heated over a water bath maintained at 80 ºC for 15 min. The extract obtained was filtered through Whatmann No1 Filter paper (pore size 25 µm) and stored in refrigerator for further experiments.

Phytochemical Screening

Tannins: 2 ml of extract and 2 ml of 5 % FeCl3 was added and observed for the formation of yellow brown precipitate.

Alkaloids: Few ml of extract a drop or two of Mayer's reagent were added by the side of the test tube. A white or creamy precipitate indicates the test as positive.

Saponins: A few ml of extract was shaken vigorously and observed for a stable persistent froth. The frothing was mixed with few drops of olive oil and shaken vigorously after which it was observed for the information of emulsion.

Terpenoids: 2 ml of extract, 1 ml of CHCl3, 2 ml of acetic acid anhydride, and concentrated H2SO4 were added carefully to form layer. Reddish brown coloration of interface was observed to detect the presence of Terpenoids.

Flavonoids: 2 ml of extract, few drops of concentrated HCl followed by 0.5 g of zinc or magnesium turnings were added. The solution was observed for the appearance of magenta red or pink color after 3 min.

Phenolics: 2 ml of extract, 1 ml of 1% ferric chloride solution was added blue color indicates phenols.

Anthraquinones: 1 ml of plant extract, few drops of 10 ammonium solution were added, appearance pink color precipitate indicates the presence of Anthraquinones.

Phytosterols: Few ml of filtrate, 2 ml of acetic anhydride, to this, one or two drops of concentrated sulphuric acid were added slowly along the sides of the test tube. An array of color changes shows the presence of phytosterols.

Coumarins: 1 ml of extract, 1 ml of 10% NaOH was added. Formation of yellow color indicates the presence of coumarins.

Anthocyanins: 2 ml of extract, 2 ml of 2N HCl was added followed by the addition of NH3. Pinkish red to bluish violet coloration indicates the presence of anthocyanins.

Glycosides: The extract was hydrolyzed with HCL solution and neutralized with NaOH solution. A few drops of Fehling's solution A and B were added. Red precipitate in indicates the presence of glycosides.

Reducing sugars: The extract was shaken with distilled water and filtered. The filtrate was boiled with drops of Fehling's solution A and B for minutes. An orange red precipitate indicates the presence of reducing sugars.

Determination of total Phenolic and Tannin Contents:

The total phenolic content was determined according to the method described by Siddhuraju and Becker [12], the tannin content of the sample was calculated as: Tannin (%) = Total phenolics (%) – Non-tannin phenolics (%).

Estimation of total Flavonoid Content

The total flavonoid content of sample extracts was determined by the use of a slightly modified colorimetric method described previously [13]. Absorbance of the mixture was determined at 510 nm versus prepared water blank. Rutin was used as a standard compound for the quantification of total flavonoid. All the values were expressed as gram of rutin equivalent (RE) per 100 gram of extract.

Metal Chelating Activity

The chelating of ferrous was estimated by the method of Dinis *et al*. [14]. Absorbance of the solution was then measured spectrophotometric ally at 562 nm. The chelating activity of the extracts was evaluated using EDTA as standard. The results were expressed as mg EDTA equivalent/g extract.

Phosphomolybdenum Assay

The antioxidant activity of samples was evaluated by the green phosphomolybdenum complex formation according to the method of Prieto *et al*. [15]. The absorbance of the mixture was measured at 695 nm against a blank. The results reported (Ascorbic acid equivalent antioxidant activity) are mean values expressed as g of ascorbic acid equivalents/100 g extract.

Assay of Superoxide Radical Scavenging Activity:

The assay was evaluated based on the capacity of various extracts to inhibit formazan formation by scavenging the superoxide radicals generated in riboflavin–light–NBT system [16]. The absorbance was measured at 590 nm. The percentage inhibition of superoxide anion generation was calculated as: % Inhibition = [(A0 - A1)/ A0] X 100, where A0 is the absorbance of the control, and A1 is the absorbance of the sample extract/standard.

Assay of Nitric Oxide Scavenging Activity

The procedure used in the experiment according to the previous study [17]. The absorbance of the chromophore formed was read at 546 nm.

Hydrogen Peroxide Scavenging Activity

The ability of the extracts to scavenge hydrogen peroxide was determined according to the method of Ruch *et al*. [18]. Absorbance of hydrogen peroxide at 230 nm was determined, the percentage inhibition activity was calculated from [(A0 - A1)/A0] X100, where A0 is the absorbance of the control (reaction mixture without extract) and A1 is the absorbance of the extract/standard.

Hydroxyl Radical Scavenging Activity

The scavenging activity of chloroform, acetone, methanol and hot water extracts of H. herbacea and N. alata on hydroxyl radical was measured according to the method of Klein *et al*. [19]. The intensity of the color formed was measured spectroscopic ally at 412 nm against reagent blank. The % hydroxyl radical scavenging activity (HRSA) is calculated by: % HRSA = from [(A0 - A1)/A0] X100, where A0 is the absorbance of the control and A1 is the absorbance of the extract/standard.

Free Radical Scavenging Activity on DPPH

The antioxidant activity of the extracts was determined in terms of hydrogen donating or radical scavenging ability using the stable radical DPPH, according to the method of Blios [20]. The absorbance of the sample was measured at 517 nm. Radical scavenging activity was expressed as the inhibition percentage of free radical by the sample and was calculated by: % DPPH radical scavenging activity = (Control OD – Sample OD / Control OD) X 100.

Synthesis of Iron Oxide Nanoparticles using Leucas Aspera Leaf Extracts

The leaf extract was synthesized foe iron oxide according to Pattanayak and Nayak, and the nanoparticles were dried in oven at 80°C and stored in air tight container for further analysis.

Micro Biological Tests:

The standard microbiological tests such as Gram's staining followed by Morphological characterization and biochemical characterization tests such as Carbohydrate fermentation test, Starch utilization, Catalase test, Voges - Proskauer test, Urease test, Oxidase test, Gelatin liquefaction and Motility test were performed to identify the organism [21].

Antibacterial Assay

The standard antibacterial assays such as Agar well diffusion method [22], Antimicrobial screening by disk diffusion technique [23], Minimal Inhibitory Concentration (MIC) (Broth Tube Dilution Method) were performed.

Characterization Techniques

Characterization of the synthesized iron oxide nanoparticles and composites were carried out by different techniques. UV-VIS absorption spectrum was recorded in the region 190-1100 nm using a Perkin Elmer (Model: Lambda 35, path length of 1.0 cm, scan rate 1920 nm/sec) UV-Vis-NIR Spectrometer. The FTIR spectra were recorded using Perkin Elmer RX1 and Nicolet Avatar Model spectrophotometers in the range of 4000-400 cm–1 at a resolution of 4 cm−1 based on KBr pellet technique. X-Ray Diffraction (XRD) patterns were recorded with a PAN alytical Philips X'Pert Pro X-ray diffractometer using CuKα radiation (λ = 1.5406 A) low angle diffract grams were recorded in the 2θ range 5.0 - 80° with a 2θ step size of 0.02° and a step time of 20 second at each point. The surface morphologies were characterized by scanning electron microscopy (SEM) using JEOL JSM-6390 and FEI Quanta 200 scanning electron microscopes at an accelerating voltage of 20 keV. The elemental analysis was examined by energy dispersive X-ray analyzer (EDAX) system (Model: Oxford INCA Penta FET X3) and HPLC, LC-2030 3D model (Low pressure quaternary gradient system) was used with inbuilt PDA detector. Shimadzu LAB SOLUTIONS software (ver. 5.8) was used to operate the HPLC.

Scanning Electron Microscopy

The scanning electron microscope (SEM) uses a focused beam of high-energy electrons to generate a variety of signals at the surface of solid specimens. The signals that derive from electron-sample interactions reveal information about the sample including external morphology (texture), chemical composition, and crystalline structure and orientation of materials making up the sample. In most applications, data are collected over a selected area of the surface of the sample, and a 2-dimensional image is generated that displays spatial variations in these properties. Areas ranging from approximately 1 cm to 5 microns in width can be imaged in a scanning mode using conventional SEM techniques (magnifications ranging from 20X to approximately 30,000X with spatial resolution of 50 to 100 nm).

III. Results and Discussion

Phytochemical Analysis

Preliminary phytochemical analysis for *Leucas aspera* leaf extract was done using standard test procedures to confirm the availability of active phytochemicals in the aqueous leaf extract. The healthful properties of edible plants are perhaps due to the presence of a variety of phytoconstituents such as polysaccharides, flavonoids, glycosides, phenols, saponins, tannins etc. The preliminary screening tests are useful in the detection of these bioactive constituents. The results of phytochemical screening depicted in Table 1.

Table 1. Preliminary Phytochemical screening tests of *Leucas aspera* leaf extract

Plant Metabolite	*Leucas aspera* Aqueous Extract
Tannins	+
Alkaloids	+
Saponins	+
Terpenoids	-
Flavonoids	+
Phenolics	+
Anthraquinones	+
Phytosterols	+
Coumarins	-
Anthocyanins	+
Reducing Sugar	+
Glycosides	+

+ Presence, - Absence

Synthesis of Iron Oxide-Nanoparticles (Visual Inspection)

In the typical synthesis of iron oxide nanoparticles,

Leucas aspera leaf extract was added slowly into FeCl3 solution at room temperature. After adding the leaf extract into FeCl3 solution, within 3 min, a visible color change was observed, the yellow color aqueous solution of FeCl3 turned to greenish black indicating the synthesis of Iron oxide nanoparticles.

Antioxidant Activity of Leucas Aspera

The results of Antioxidant activity of *Leucas aspera* depicted in the following Tables 2 to 9.

Table 2. Total phenolics, tannin and flavonoid contents in hot water extracts of *Leucas aspera*

Concentration of the sample (µg/ml)	Total phenolics (mg GAE / gm extract)	Tannin (mg GAE/ gm extract)	Total Flavonoids (mg RE / gm extract)
10	50.48	175.71	280.67
20	56.67	190.95	295.33
30	62.38	208.10	306.00
40	72.86	240.00	311.33
50	84.76	244.29	317.33
60	100.48	250.00	344.67
70	108.10	262.38	348.67
80	115.24	312.86	381.33
90	117.14	372.38	394.00
100	124.29	559.05	399.33

GAE; Gallic acid equivalent, RE; Rutin equivalent.

Table 3. Total phenolics, tannin and flavonoid contents in acetone extracts of *Leucas aspera*

Concentration of the sample (µg/ml)	Total phenolics (mg GAE / gm extract)	Tannin (mg GAE/ gm extract)	Total Flavonoids (mg RE / gm extract)
10	45.71	19.52	44.67
20	87.14	21.43	72.67
30	101.43	61.43	114.67
40	145.24	101.90	132.00
50	153.33	119.52	166.00
60	162.86	130.95	247.33
70	177.62	157.62	261.33
80	195.71	188.57	327.33
90	226.67	194.76	341.33
100	232.86	218.10	384.67

GAE; Gallic acid equivalent, RE; Rutin equivalent

Table 4. Metal chelating, Phosphomolybdenum and super oxide radical scavenging activity of hot water extracts of *Leucas aspera*

Concentration of the sample (µg/ml)	Metal chelating activity (mg EDTAE / gm extract)	Phosphomolybdenum activity (mg AAE/ gm extract)	Superoxide Radical Scavenging (%)
10	10.48	23.11	15.29
20	11.38	26.22	20.13
30	12.52	27.39	23.27
40	13.48	28.33	27.16
50	15.00	30.50	28.68
60	15.79	36.44	40.84
70	16.93	37.39	47.67
80	18.03	42.28	50.52
90	19.10	43.67	86.04
100	19.90	45.67	87.46

EDTAE: Ethylene diamine tetra acetic acid equivalent; AAE: Ascorbic acid equivalent.

Table 5. Metal chelating, Phosphomolybdenum and super oxide radical scavenging activity of acetone extracts of Leucas aspera

Concentration of the sample (µg/ml)	Metal chelating activity (mg EDTA / gm extract)	Phosphomolybdenum activity (mg AAE/ gm extract)	Superoxide Radical Scavenging (%)
10	4.28	2.89	50.62
20	6.93	5.78	53.75
30	7.76	9.22	53.94
40	9.86	10.17	61.92
50	10.66	14.56	69.52
60	11.24	15.11	71.98
70	12.79	17.72	74.26
80	13.10	23.06	86.23
90	13.69	24.67	88.51
100	14.00	28.67	90.69

EDTAE: Ethylene diamine tetra acetic acid equivalent; AAE: Ascorbic acid equivalent.

Table 6. Nitric Oxide Scavenging, Hydrogen Peroxide Scavenging and Hydroxyl Radical Scavenging activity of hot water extracts of *Leucas aspera*

Concentration of the sample (µg/ml)	Nitric Oxide Scavenging (%)	Hydrogen Peroxide Scavenging (%)	Hydroxyl Radical Scavenging (%)
10	56.70	34.76	13.01
20	56.79	36.66	20.42
30	60.02	39.98	22.51
40	63.44	43.21	23.17
50	71.04	50.43	24.12
60	77.21	57.36	24.79
70	77.78	60.87	29.53
80	80.91	62.77	33.81
90	83.76	79.49	36.28
100	88.79	89.36	36.28

Table 7. Nitric Oxide Scavenging, Hydrogen Peroxide Scavenging and Hydroxyl Radical Scavenging activity of acetone extracts of Leucas aspera

Concentration of the sample (µg/ml)	Nitric Oxide Scavenging (%)	Hydrogen Peroxide Scavenging (%)	Hydroxyl Radical Scavenging (%)
10	55.94	14.53	17.76
20	60.87	56.51	22.51
30	63.06	60.02	29.82
40	71.51	68.38	32.38
50	73.41	73.79	34.28
60	75.78	74.93	36.94
70	75.97	77.30	39.70
80	79.68	84.90	41.98
90	81.77	89.36	43.68
100	83.48	92.97	51.00

Table 8. DPPH Scavenging activity of hot water extracts of *Leucas aspera*

Concentration of the sample (µg/ml)	DPPH Scavenging (%)
10	38.06
20	44.57
30	48.50
40	52.84
50	57.29
60	58.84
70	64.32
80	75.80
90	79.52
100	86.66

Table 9. DPPH Scavenging activity of acetone extracts of *Leucas aspera*

Concentration of the sample (µg/ml)	DPPH Scavenging (%)
10	7.96
20	11.58
30	17.17
40	19.44
50	28.54
60	29.47
70	32.16
80	45.92
90	50.57
100	59.05

The antibacterial properties of the Iron oxide Nanoparticles were evaluated against Gram positive and Gram negative bacterial strains using agar well diffusion method. Chart 1 shows the effect of Iron oxide nanoparticles on the growth of both Gram positive and Gram negative bacteria. Iron oxide nanoparticles exhibited significant antibacterial activity against Gram positive bacteria than Gram negative pathogenic bacterial strains tested.

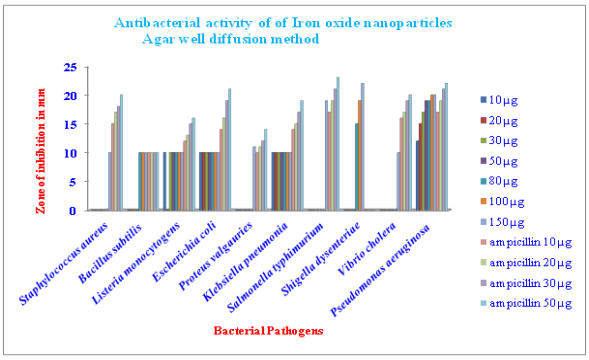

Chart 1. Effect of Iron oxide nanoparticles on the growth of Gram positive and Gram negative bacteria

Of the bacterial stains tested, Iron oxide nanoparticles strongly inhibited the growth of Gram positive bacteria - *Bacillus cereus (10 mm), Staphylococcus aureus (10 mm) and Listeria monocytogens (10 mm) at a concentration of 150 µg.* On the other hand, Iron oxide nanoparticles moderately inhibited the growth of Gram negative bacteria- *Escherichia coli (10 mm) and Klebsiella pneumoniae (10 mm), Proteus mirabilis (11 mm), Salmonella enterica (19 mm) , Shigella flexneri (22 mm), Vibrio cholera (10 mm) and Pseudomonas aeuroginosa (20 mm)* at a concentartion of 150 µg. These nanoparticles showed a low inhibitory effect on the growth of Bacillus cereus (10 mm).

Antibacterial activity results of leaf extract of L. aspera were given in chart 2. In general, the mean zone of inhibition produced by the commercial antibiotic, ampicillin, was between 10.0 to 13.0 mm and was larger than those produced by leaf extracts which was between 10.0 to 21.0 mm. *Bacillus cereus (No zone formation), Staphylococcus aureus (11 mm) and Listeria monocytogens (12 mm) at a concentration of 150 µg.* On the other hand, Iron oxide nanoparticles moderately inhibited the growth of Gram negative bacteria- *Escherichia coli (12 mm) and Klebsiella pneumoniae (10 mm), Proteus mirabilis (17 mm), Salmonella enterica (21 mm), Shigella flexneri (20 mm), Vibrio cholera (12 mm) and Pseudomonas aeuroginosa (21 mm)* at a concentartion of 50 µg. These nanoparticles showed a low inhibitory effect on the growth of Bacillus cereus (No zone formation).

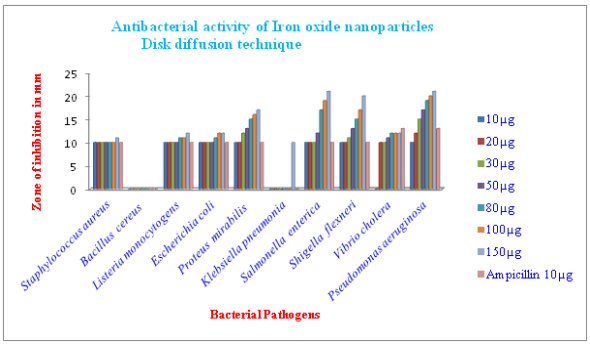

Chart 2. Antibacterial activity results of leaf extract of L. aspera

Minimum inhibitory concentration of Iron oxide Nanoparticles for the antibacterial activities was presented in chart 3. The Minimal Inhibitory Concentration produced by the commercial antibiotic, ampicillin, was between 500 µg and was larger than those produced by leaf extracts which was between 500 – 2000 µg.

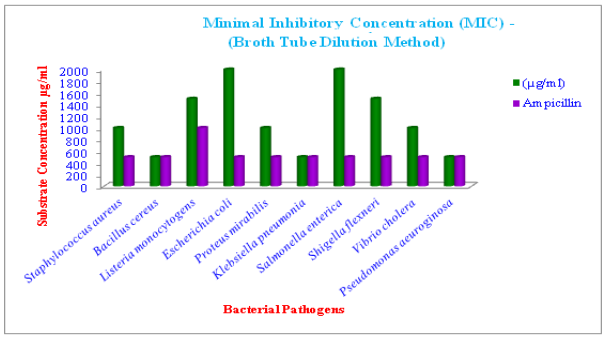

Chart 3. MIC value of Iron oxide Nanoparticles for the antibacterial activities

The optical property of synthesized iron oxide nanoparticles is one of the important characteristics for evaluation of its optical and photo catalytic activity. UV-Visible absorption spectrum is the preliminary characterization to know the optical property. The result obtained from UV-Visible spectroscopy analysis of the sample is presented in Figure 1.

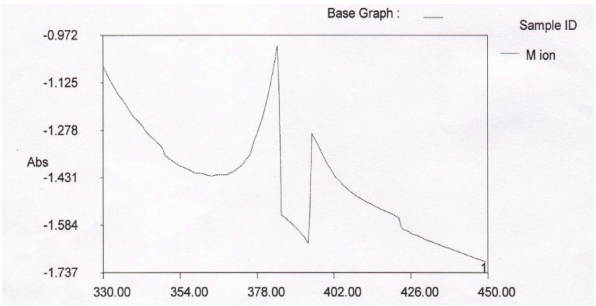

Fig. 1. UV-Vis spectrum of Iron oxide nanoparticles synthesized using *Leucas aspera* leaf extract

International Journal of Agriculture Innovations and Research
Volume 6, Issue 2, ISSN (Online) 2319-1473

FTIR spectra of biosynthesized Iron oxide nanoparticles were recorded to identify the capping and efficient stabilization of metal nanoparticles by functional groups of biomolecules present in *Leucas aspera* leaf extract. Figure 2 shows the FT-IR spectrum of prepared iron oxide nanoparticles.

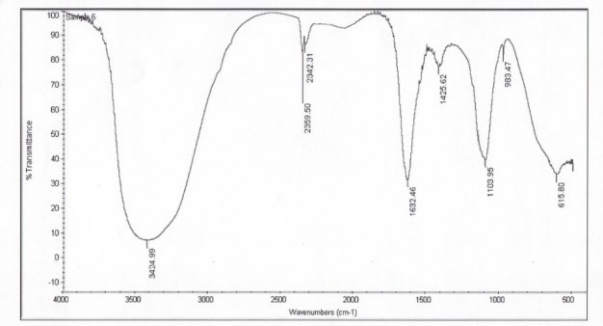

Fig. 2. FTIR spectrum of Iron oxide nanoparticles synthesized using *Leucas aspera* leaf extract

The phase identification and crystalline structure of the nanoparticles were characterized by X-ray diffraction. The X-ray diffraction patterns obtained for the Fe3O4 - NPs synthesized using *Leucas aspera* extract is shown in Figure 3.

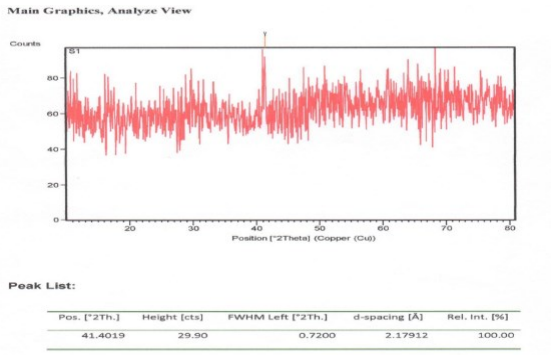

Fig. 3. XRD pattern of Iron oxide nanoparticles synthesized using *Leucas aspera* leaf extract

SEM images revealed that the synthesized iron oxide nanoparticles were aggregated as irregular rhombic shapes with panoramic view and range from 117 µm -1.29 mm in size (Figure-4 A-4D).

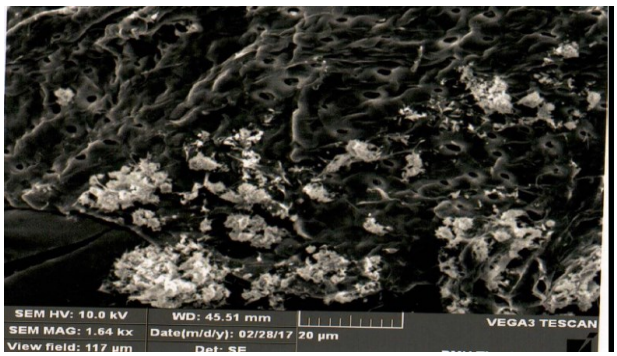

Fig. 4A. SEM images of Iron oxide nanoparticles synthesized using *Leucas aspera* leaf extracts at 117µm magnification levels

Fig. 4B. SEM images of Iron oxide nanoparticles synthesized using *Leucas aspera* leaf extracts at 410µm magnification levels

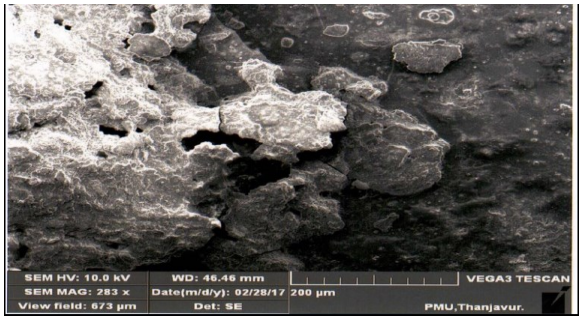

Fig. 4C. SEM images of Iron oxide nanoparticles synthesized using *Leucas aspera* leaf extracts at 673µm magnification levels

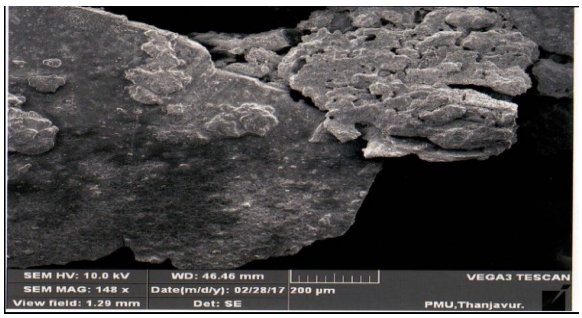

Fig. 4D. SEM images of Iron oxide nanoparticles synthesized using *Leucas aspera* leaf extracts at 1.29 mm magnification levels

The proposed optimization of extraction conditions for HPLC method can be used to develop a fingerprint for the identification of *Leucas aspera* leaf extract Figure 5.

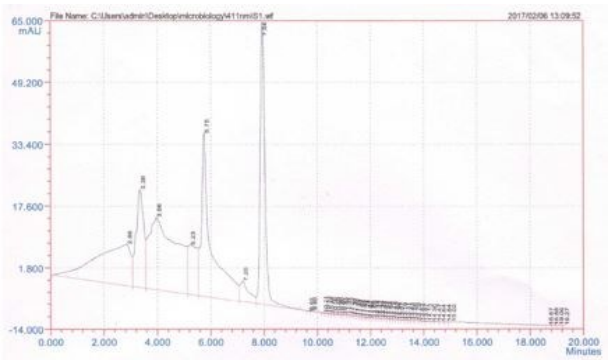

Fig. 5. HPLC - pattern of Iron oxide nanoparticles synthesized using *Leucas aspera* leaf extract

Some authors have demonstrated that the small size of nanoparticles can also contribute to bactericidal effects. For example, Lee *et al*. [24] Reported that the inactivation of Escherichia coli by zero valent iron nanoparticles could be because of the penetration of the small particles (sizes ranging from 10 - 80 nm) into *E. Coli* membranes. Nano scale zero valent iron (NZVI) could then react with intracellular oxygen, leading to oxidative stress and eventually causing disruption of the cell membrane. Studies on ZnO and MgO nanoparticles have also shown that antibacterial activity increased with decreasing particle size. In the present study, the concentration of nanoparticles was a major factor for antibacterial activity of the nanoparticle. A similar concentration dependent behavior was observed by Kim *et al*. [25] when they investigated the antimicrobial effects of Ag and ZnO nanoparticles on *S. aureus* and *E. coli*. Similarly, in a study of bactericidal effects of iron noxide nanoparticles on *S. epidermidis*, Taylor and Webster also reported concentration dependent bacterial inhibition. It is also important to note that IO nano particles do not negatively influence all cells and thus it can be said that with an appropriate external magnetic field, FeO nanoparticles may be directed to kill bacteria as needed throughout the body.

Generally, the iron oxide nanoparticles have been prepared by strong hydrolysis of iron salts at elevated temperature [26]. The plant mediated iron oxide nanoparticles were prepared at room temperature. Hence the mechanism of study of iron oxide nanoparticles formation is a little difficult. However, the organic compound, which is present in the plant extract, acts as a reducing as well as capping or binding agent to form iron oxide nanoparticles. The colour change arise from the excitation of the surface plasman resonance (SPR) phenomenon is typically of iron oxide nanoparticles [27].

Most of the synthetic antibiotics now available in the market have major setback due to the multiple resistance developed by pathogenic microorganisms against their drugs [28]. The emergence of Nano science and nanotechnology in the last decade presents opportunities for exploring the bactericidal effect of metal nanoparticles. The bactericidal effect of metal nanoparticles has been attributed to their small size and high surface to volume ratio, which allows them to interact closely with microbial membranes and is not merely due to the release of metal ions in solution [29].

Kiruba Daniel *et al*., [30] used leaf extract of the evergreen shrub Dodonaea viscosa to synthesize iron nanoparticles and the antimicrobial activity of synthesized nanoparticles was evaluated against human pathogens, namely, *E. coli, K. pneumoniae, P. fluorescens, S. aureus, and B. subtilis*. A very low concentration of as-synthesized nanoparticles was sufficient to display effective antimicrobial activity as compared to earlier reports. Senthil and Ramesh [9] reported the green synthesis of Fe3O4 nanoparticles at room temperature using leaf extract of Tridax procumbens and the synthesized nanoparticles were effective against *Pseudomonas aeruginosa*. The zone of inhibition increased from 1 mm to 2 mm when the concentration of nanoparticles increased fourfold. Nanoparticles prepared by using *Abelmoschus esculentus* as a reducing and capping agent significantly inhibited the growth of *Escherichia coli* and *Staphylococcus aureus*.

Bacterial strains were spread on agar plates. Different amounts of Fe3O4 nanoparticles (25 µg and 50 µg) were placed in the wells. Controls contained Ampicillin (20 µg) in place of Fe3O4 nanoparticles. The incubation period was 24 h at 37^0C. Zone of inhibition was measured as described in methods.

Bacterial strains were spread on agar plates. Different concentrations of Iron oxide nanoparticles (0.1-2.0 mg/ml) were placed in the wells. Control contained Ampicillin (20 µg) in the place of nanoparticles. The incubation period was 24 h at 37^0C. Zone of inhibition was measured and minimum inhibitory concentration of Iron oxide nanoparticles was determined.

Addition of *Leucas aspera* extract to 0.001 M ferric (III) chloride produced an instantaneous color change in the solution from yellow to intense brown, indicating the formation of iron-containing nanoparticles [31]. This phenotypic change correlated well with the absorption spectra data, such that the absorption peak at 360 nm of the ferric (III) chloride was shifted to 405 nm after the addition of the plant extract, with the 405 nm peak being indicative of iron nanoparticle formation.

In the present study, the absorption maxima of synthesized Iron oxide nanoparticles are similar to those observed in other studies which used tea and sorghum extracts to produce iron nanoparticles [31-33]. An absorption maxima of iron nanoparticles with a peak of 415 nm has been reported [34-35].

In the figure 2 shows the FT-IR spectrum of prepared iron oxide nanoparticles. It displays three strong bands around 3468 cm −1 (br), 1626 cm −1 and 548 cm −1. The observed bands are nearer to those reported for Iron nanoparticles [36]. The vibration bands are 615 cm −1 (Fe –O stretching), 1632 cm −1 (H2O bending vibration) and a broad peak at 3424 cm −1 (H2O stretching) indicating phenolic compounds. Presence of organic molecule on the surface of iron oxide nanoparticles has the influence on the FT-IR peaks [24].

The broad peak observed around 548 cm −1 (Fe –O stretching) instead of two sharp peaks, may be due to the organic molecule which was from the leaf extract on the surface of iron oxide nanoparticles. The weak band at 2074 cm −1 may be due to the unsaturated Nitrogen (C ≡ N) compounds, tannins and alkaloids from the leaf extract. Based on these results, the presence of phenolic compounds, tannins and alkaloids were believed to be responsible for the formation and stabilization of synthesized iron oxide nanoparticles in plants, the secondary metabolism products, such as flavonoids, flavones, isoflavones, isothiocyanates, carotenoids, polyphenols that have potent biological activities are known as an important natural resource for the synthesis of metallic nanoparticles [37]. Flavonoids in Dodonaea viscosa leaf extract were identified to be responsible for the reduction of metal salt to synthesize iron oxide nanoparticles along with polyhydroxy groups in santin, tannins and saponins which were considered to be acting as capping agents based on

FTIR analysis [30]. Similarly, the presence of phenols, flavonoids, alkaloids, saponins, cardiac glycosides, steroids, carbohydrate and proteins in Tinospora cordifolia were reported to be responsible for the reduction of Ferric ions into nano forms.

Senthil and Ramesh [9] reported that carbohydrates present in the Tridax procumbens plant extract were responsible for Fe3O4 nanoparticle synthesis at room temperature. The phytochemical screening of Tridax procumbens revealed the presence of alkaloids, carotenoids, flavonoids, saponins and tannins [38] and reported to be responsible for the Fe3O4 nanoparticle synthesis.

The synthesized particles when subjected to XRD analysis, gave a clear picture on the presence of major characteristic peaks for prepared crystalline metallic nanoparticles at 2θ values of 24.2, 33.1, 35.7, 40.9, 49.4, 54.1, 57.6, 62.6, and 64.0 degrees corresponding to (14), (102), (112), (115), (21), (113), (012), (218), and (298) respectively. In addition, the peak observed at 2θ values of 45.5 is corresponding to (335). It might be due to the presence of trace amount of hollow –Fe3O4 nanoparticles. It indicates that the prepared iron oxide nanoparticles are well crystalline. Above all, it is encouraging to note that the 2θ values of the synthesized iron oxide nanoparticles are also matched with Joint Committee for Powder Diffraction Standard (JCPDS) which are in rhombohedral geometry.

The XRD spectrum obtained with the Iron oxide nanoparticles synthesized using *Leucas aspera* leaf extract showed three different diffraction peaks corresponding to the crystal planes of crystalline Fe2O3. The sharp peaks indicated the crystallinity and purity of iron oxide nanoparticles [39]. Phumying *et al*., [40] reported the synthesis Fe3O4 nanoparticles using Aloe vera plant extract and high purity of synthesized nanoparticles was confirmed with XRD. The average particle size calculated from XRD increased with an increase in temperature and time. Based on the cocercivity, it was concluded that the nanoparticles were super paramagnetic in nature.

To find out the purity of the metal particles synthesized, EDX spectrum was obtained. Dispersive X-ray Spectroscope (EDX) analysis showed the presence of elemental iron oxide signal in the sample. The appearance of chloride and carbon in the EDX spectrum is because of the FeCl3 precursors used in the synthesis protocol and attributed mainly to organic molecules in the leaf extract.

Iron oxide nanoparticles synthesized by using the leaf extract of Carica papaya showed that the synthesized nanoparticles were plate like structures with coarsened grains, uniformly distributed small spherical shaped particles and at higher magnification, large number of homogeneous nanocapsule like morphology of iron oxide nanoparticles were observed [41]. In the previous studies reported that the typical SEM image revealed that the iron nanoparticles were clearly distinguishable at different enlargements were found to be polydispersed and measured in size from 24 to 34 nm.

An eco-friendly green synthesis of iron oxide nanoparticles using leaf extract of *Leucas aspera* revealed that the particles were aggregated with rough surfaces. Transmission electron microscope image of iron oxide nanoparticles showed that the nanoparticles size was below 20 nm.

It is revealed that in 10 µL of *Leucas aspera* leaf extract, there are 15 peaks at the Rt 3.680, 3.783, 4.740. 5.064, 5.234, 5.580, 6.176, 7.287, 8.030,8.723, 8.523, 9.679, 11.063,11.259 and 12.626 are indicating the occurrence of at least 15 different components in 10 µL leaf extract.

IV. Conclusion

Recent advances in nanoscience and nanotechnology have also led to the development of novel nanomaterials, which ultimately increase potential health and environmental hazards. Interest in developing environmentally benign procedures for the synthesis of metallic nanoparticles has been increased. The purpose is to minimize the negative impacts of synthetic procedures, their accompanying chemicals and derivative compounds. The exploitation of different biomaterials for the synthesis of nanoparticles is considered a valuable approach in green nanotechnology. The present study proved that the biological approach of synthesis of Iron oxide nanoparticles using *Leucas aspera* leaf extract appears to be ecofriendly and cost effective alternative to conventional chemical and physical methods and would be suitable for developing large scale production. Consequently, the green synthesis using *Leucas aspera* leaf extracts can be economic and effective method for the synthesis of iron oxide nanoparticles. Therefore this simple, low cost and greener method for development of nanoparticles may be valuable in environmental, biotechnological and biomedical applications.

References

[1] Thakkar, K.N., Mhatre, S.S., Parikh, R.Y. Biological synthesis of metallic nanoparticles. Nanomedicine. 2010, 6(2): 257–262.

[2] Panigrahi S., Kundu, S., Ghosh, S.K., Nath, S., Pal, T. General method of synthesis for metal nanoparticles. J. Nanoparticle Res., 2004, 6(4): 411–414.

[3] Ahmad, N., Sharma, S., Singh, V.N., Shamsi, S.F., Fatma, A., Mehta, B.R. Biosynthesis of Silver Nanoparticles from Desmodiumtriflorum: a novel approach towards weed utilization.," Biotech. Res. 2011, Int. 1- 8.

[4] Gardea-Torresdey, J.L., Parsons, J.G., Gomez, E. Formation and growth of Au nanoparticles inside live Alfalfa plants. Nano Lett., 2002, 2(4): 397– 401.

[5] Rai, M., Yadav, A., Gade, A. CRC 675 — current trends in phytosynthesis of metal nanoparticles. Critic. Rev. Biotechnol., 2008, 28(4): 277–284.

[6] Vicky, M., Rodney, S., Ajay, S., Hardik, M. Introduction to metallic nanoparticles. J. Pharm. Bioallied Sci., 2010, 2(4): 282-289.

[7] Yeary, L.W., Ji, W.M., Love, L.J., Thompson, J.R., Rawn, C., Phelps, J., Tommy, J. Magnetic properties of biosynthesized magnetite nanoparticles, Magnetics, IEEE Transac., 41: 4384-4389. Pharm. Bioallied Sci., 2005, 2(4): 282-289.

[8] Roh, H., Vali, T., Phelps, J., Moon, J.W. Extracellular synthesis of magnetite and metal-substituted magnetite nanoparticles, J. Nanosci Nanotechnol., 2006, 6:3517-3520.

[9] Senthil, M., Ramesh, C. Biogenic synthesis of Fe3O4 nanoparticles using Tridaxprocumbens leaf extract and its antibacterial activity on Pseudomonas aeruginosa. J. Nanomat. Biostruc., 2012, 7: 1655-1660.

[10] Rai, M., Yadav, A. and Gade, A. Silver nanoparticles as a new

generation of antimicrobials. Biotechnol Adv, 2009, 27: 76-83.
[11] Gamble J. S., C. E. C. Fisher (1915-1936). Flora of the Presidency of Madras II Parts. Conference Proceedings, 2003.
[12] Siddhuraju, P. Becker, K., Antioxidant properties of various solvent extracts of total phenolic constituents from three different agro climatic origins of drumstick tree (Moringaoleifera Lam.) leaves. J. Agric. Food Chem., 2003, 51 (8): 2144-2155.
[13] Zhishen J, Mengcheng T and Jianming W. The determi- nation of flavonoid contents in mulberry and their scavenging effects on superoxide radicals. Food Chemistry, 1999, 64: 555 -559.
[14] Dinis TCP, Madeira VMC, Almeida MLM. Action of phenolic derivates (acetoaminophen, salycilate and 5-aminosalycilate) as inhibitors of membrane lipid peroxidation and as peroxyl radical scavengers. Arch. Biochem. Biophys. 1994, 315: 161-169.
[15] Prieto P, Pineda M and Aguilar M. Spectrophotometric quantitation of antioxidant capacity through the formation of a Phosphomolybdenum Complex: Specific application to the determination of vitamin E. Analytical Biochemistry 1999, 269: 337-341.
[16] Beauchamp, C. and Fridovich, I. Superoxide Dismutase: Improved Assays and an Assay Applicable to Acrylamide Gels. Analytical Biochemistry, 1971, 44: 276-287.
[17] Sreejayan N and Rao MNA, Nitric oxide scavenging activity by curcuminoids, J Pharm Pharmacol, 1997, 47:105-107.
[18] Ruch, R.J., Cheng, S.J., and Klaunig, J.E. P reventi- on of cytotoxicity and inhibition of intracellular communication by antioxidant catechins isolated from Chine se gre-en tea. Carcinogenesis, 1989, 10: pp. 1003-1008.
[19] Klein SM, Cohen G, Cederbaum AI. Production of formaldehyde during metabolism of dimethyl sulphoxide by hydroxyl radical generating system. Biochemistry 1991, 20: 6006- 601.
[20] Blois, M.S., Antioxidant determinations by the use of a stable free radical. Nature. 1958, 29:1199 - 1200.
[21] Gunasekaran P. Laboratory Manual in Microbiology, New Age International Pvt. Ltd. Publishers, New Delhi. 1995.
[22] Murray PR, Baron EJ, P faller MA, Tenover FC, Yolken HR Manual of Clinical Microbiology, 6th Ed. ASM Press, Washington DC, 1995; 15-18.
[23] NCCLS. Methods for dilution antimicrobial susceptibility tests for bacteria that grow aerobically. 3rd ed. Wayne, PA: NCCLS; 2002, p. M100-S12.
[24] Lee, Jiwon., Tetsuhiko, Isobe., Mamoru, Senna. Preparation of ultrafine Fe 3O4 particles by precipitation in the presence of PVA at high pH. J. Coll. Inter Sci., 1996, 177(2): 490-494.
[25] Kim, D., Lee, N., Park, M., Kim, B. H., An, K. and Hyeon, T. Synthesis of uniform ferrimagnetic magnetite nanocubes. J Am Chem Soc, 2009, 131: 454-455.
[26] Ocana, M, Morales, M.P., Serna, C.J. Homogeneous precipitation of uniform α-Fe2O3 particles from iron salts solutions in the presence of urea. J. colloid inter sci., 1999, 212 (2): 317-323.
[27] Shankar, S.S., Rai, A., Ankamwar, B., Singh, A., Ahmad, A., Sastry, M. Biological synthesis of triangular gold nanoprisms. Nat. Mater., 2004, 3(7): 482-488.
[28] Akinpelu, D.A., Aiyegoro, O.A., Okoh, A.I. In vitro antimicrobial and phytochemical properties of stem bark of Afzeliaafricana (Smith). Afri. J. Biotech., 2008, 7(20): 3665 -3670.
[29] Mohanty, L., Parida, U.K., Ojha, A.K, Nayak, P.L. Green synthesis of Gold nanoparticle using Elettaria cardamom seed extract. J. Micro Antimicro., 2011, 3:105-109.
[30] Kiruba Daniel, S.C.G., Vinothini, G., Subramanian, N., Nehru, K., Sivakumar, M. Biosynthesis of Cu, ZVI and Ag nanoparticles using Dodonaea viscosa extract for antibacterial activity against human pathogens. J. Nano Res., 2013, 15(1):1-10.
[31] Kharissova, O.V., Dias, H.V., Kharisov, B.I., Perez, B.O., Perez, V.M. The greener synthesis of nanoparticles. Trends Biotechnol., 2013, 31(4): 240−248.
[32] Njagi, E.C., Huang, H., Stafford, L., Genuino, H., Galindo, H.M., Collins, J.B., Hoag, G.E., Suib, S.L. Biosynthesis of iron and silver nanoparticles at room temperature using aqueous sorghum bran extracts. Langmuir., 2011, 27(1): 264-271.
[33] Hoag, G., Collins, A., Holcomb, J., Hoag, J., Nadagouda, M., Varma, R. Degradation of bromothymol blue by 'greener' nano-scale zero-valent iron synthesized using tea polyphenols. J. Mater. Chem., 2009, 19: 8671−8677.
[34] Madhavi, V., Prasad, T.N.V.K.V., Reddy, A.V B., Ravindra Reddy, B., Madhavi, G. Application of phytogenic zerovalent iron nanoparticles in the adsorption of hexavalent chromium. Spectrochimica Acta A: Mol. Biomol. Spectro., 2013, 116:17–25.
[35] Mazur, M., Barras, A., Kuncser, V., Galatanu, A., Zaitzev, V., Turcheniuk, K.V., Woisel, P., Lyskawa, J., Laure, W., Siriwardena, A., Boukherroub, R., Szunerits, S. Iron oxide magnetic nanoparticles with versatile surface functions based on dopamine anchors. Nanoscale., 2013, 5:2692–2702.
[36] Kumar, A., Singhal, A. Synthesis of colloidal β-Fe2O3 nanostructures-influence of addition of Co2+ on their morphology and magnetic behavior. Nanotechnol., 2007, 18(47): 1-7.
[37] Park, Y., Hong, Y.N., Weyers, A., Kim, Y.S., Linhardt, R.J. Polysaccharides and phytochemicals: a natural reservoir for the green synthesis of gold and silver nanoparticles. IET Nanobiotechnol., 2011, 5: 69-78.
[38] Ikewuchi, J.C., Ikewuchi, C.C., Igboh, M.N. Chemical profile of Tridax procumbensLinn. Pak. J. Nutr., 2009, 8(5): 548-550.
[39] Balamurughan, M.G., Mohanraj, S., Kodhaiyolii, S., Pugalenthi, V. Ocimum sanctum leaf extract mediated green synthesis of iron oxide nanoparticles. Spectroscopic and microscopic studies. J. Chem. Pharm. Sci., 2014, 4: 201–204.
[40] Phumying, S., Labuayai, S., Thomas, C., Amornkitbamrung, V., Swatsitang, E., Maensiri, S. Aloe vera plant-extracted solution hydrothermal synthesis and magnetic properties of magnetite (Fe3O4) nanoparticles. Applied Physics A., 2013, m111(4):1187–1193.
[41] Latha, N., Gowri, M. Biosynthesis and characterization of Fe3O4 nanoparticles using Carica papaya leaves extract. Int. J. Sci. Res., 2014, 3(11): 1551-1556.

AUTHORS' PROFILES

Dr. V. Veeramanikandan
Is the Assistant Professor in Research Centre in Microbiology of MGR College, Hosur. He has more than 12 years of teaching and research experience with specialization in Nanotechnology and Bioplastics Production. He is the mentor for 5 Ph D Scholars and had guided more than 30 M. Phil and M. Sc students. Dr. V. Veeramanikandan has gained considerable expertise in microbiological and molecular biological techniques during the past decade. He has also specialized himself with techniques like molecular characterization of microbes, protein purification, 2D gel electrophoresis, HPLC etc. Apart from this, he has expertise in biological techniques such as DNA and RNA isolation from tissues and in working with nucleic acids.

Madhu G. C,
Research Scholar, PG & Research Centre in Microbiology, Dr. M.G.R. Nagar, Hosur, Krishnagiri (District), Tamilnadu, India. Pin - 635 109.

Pavithra V,
Post graduate Student, PG & Research Centre in Microbiology, Dr. M.G.R. Nagar, Hosur, Krishnagiri (District), Tamilnadu, India. Pin - 635 109.

Jaianand Kannaiyan
Research Scholar, PG & Research Centre in Biotechnology, Dr. M.G.R. Nagar, Hosur, Krishnagiri (District), Tamilnadu, India. Pin - 635 109.

Dr. P. Balaji
Is the Head in PG and Research Centre in Biotechnology of MGR College, Hosur. An eminent Scientist having gained over 13 year of rich experience in managing collaborative and independent research functions. An esteemed academician having the distinction of being associated with numerous Scientific Seminars, Presentations, Workshops, Talk Invitations, Conferences as well as publishing of a plethora of Articles & Papers. He Possesses expertise knowledge in Cancer Biology, Enzymology, Microbial Biochemistry, Nutriceuticals and Secondary metabolites.